AD-A248 414

FINAL REPORT
OFFICE OF NAVAL RESEARCH

GRANT NUMBER: N00014-90-J-1588

EVALUATION OF AN ANALYTICAL MODEL
FOR
PREDICTING LIGHT SCATTERING FROM
CYLINDRICALLY-SHAPED OBJECTS
IN THE OCEAN

Principal Investigator:

Patricia G. Hull
Tennessee State University

March 5, 1992

92   ᴶ ʋᴜ 213

92-08696

TITLE: EVALUATION OF AN ANALYTICAL MODEL FOR PREDICTING LIGHT
SCATTERING FROM CYLINDRICALLY SHAPED OBJECTS IN THE OCEAN

SUMMARY

The polarization state of light in the ocean can be used to enhance visibility. We are investigating the consequences of scattering from non-spherically-symmetric particles on light propagation and visibility in the ocean. To calculate scattering from non-spherical marine micro-organisms, it is usually necessary to resort to approximate methods. One promising approximation is the coupled-dipole approach in which an arbitrarily-shaped object is divided into a number of identical elements arranged on a cubic lattice. Each element is treated as a spherical, dipolar oscillator with its polarizability specified by the real and imaginary parts of the index of refraction. Interactions between dipoles are included by determining the field at a particular dipole due to the incident field and the fields induced by the other dipole oscillators. The scattered field is then the sum of the fields due to each oscillator. The coupled-dipole method is promising because, in principle, an organism of any shape can be modelled, and all sixteen elements of the scattering matrix calculated. We have applied this approach to calculate scattering from spherical particles to verify the limits of the approximation, and from other shapes to investigate the effects of non-sphericity and chirality on scattering. In particular, we calculated all 16 Mueller matrix elements for the scattering from a finite cylinder, a single-strand helix, 14-strand helix, and ensembles of these particles. The effects of pitch, size, wavelength, and complex index of refraction were investigated. The results provide insights into the magnitude and type of depolarization effects associated with various marine micro-organisms containing these structures.

1. RESEARCH GOALS

The long term goal of this project is to understand and quantify the consequences of light scattering from ensembles of irregularly-shaped objects with varying degrees of orientation on the optical preperties of the ocean and the transmission of polarized light through sea water.

2. OBJECTIVES

The primary objective of the project is to develop an analytical model to predict light scattering from randomly- oriented non-spherical marine micro-organisms. The effects of these particles on the transmission of polarized light through sea water is examined by studing the symmetry and angular variability of the Mueller scattering matrix elements calculated from the model.

3. APPROACH

The treatment of the general problem of light scattering from a small particle in the text by Bohren and Huffman[1] provides a convenient method for analyzing the polarization properties of light scattered by small particles. The complete polarization properties of a beam of light can be described by a four element Stokes vector $F = [I,Q,U,V]$, where I is the total intensity of light, Q represents vertical or horizontal polarization, U represents 45° polarization, and V represents circular polarization. In this formalism, the effect of a scattering medium on the beam may be represented by the matrix equation, $F' = M\,F$, shown in terms of the matrix elements below:

$$
\begin{bmatrix} I_s \\ Q_s \\ U_s \\ V_s \end{bmatrix} = \frac{1}{k^2 r^2} \begin{bmatrix} S_{11} & S_{12} & S_{13} & S_{14} \\ S_{21} & S_{22} & S_{23} & S_{24} \\ S_{31} & S_{32} & S_{33} & S_{34} \\ S_{41} & S_{42} & S_{43} & S_{44} \end{bmatrix} \begin{bmatrix} I_i \\ Q_i \\ U_i \\ V_i \end{bmatrix} \tag{1}
$$

The matrix **M** (with elements S_{ij}) is known as the Mueller or 'scattering' matrix. The subscripts i and s represent incident and scattered light, respectively. The elements of the scattering matrix depend on the scattering angle and contain all the elastic scattering information available at a given wavelength. They are functions of the size, structure, symmetry, orientation, complex refractive index, and ordering of the scatterers. Generally, an evaluation of the elements of the Mueller matrix by scattering theory is based on the analytical solution to Maxwell's wave equation for the electric field as a boundary value problem. If the scattering object is a sphere or an 'infinite' cylinder and homogeneous, the analytical solutions are exact, and numerical values of the matrix elements can be calculated from these analytical solutions for the electric field by using a computer. The components of the Stoke's vector are defined in terms of the time-averaged components of the electric field perpendicular ($E_\perp$) and parallel ($E_{//}$) to the scattering plane by the relationships below.

$$
I_s = <E_{//s}E_{//s}{}^* + E_{\perp s}E_{\perp s}{}^*>
$$

$$
Q_s = <E_{//s}E_{//s}{}^* - E_{\perp s}E_{\perp s}{}^*> \tag{2}
$$

$$
U_s = <E_{//s}E_{\perp s}{}^* + E_{\perp s}E_{//s}{}^*>
$$

$$
V_s = i<E_{//s}E_{\perp s}{}^* - E_{\perp s}E_{//s}{}^*>
$$

If a particle is illuminated by a plane wave travelling in the z-direction and the scattered light is detected at a point **r**, the scattering plane is that containing **r** and **z**. The incident and scattered fields can be written in terms of a basis set of **z** and unit vectors perpendicular and parallel to the scattering plane. See figure 1 for the geometry. The incident and scattered fields are related by the matrix equation;

$$
\begin{bmatrix} E_{//s} \\ E_{\perp s} \end{bmatrix} = \frac{e^{ik(r-z)}}{-ikr} \begin{bmatrix} A_{11} & A_{12} \\ A_{21} & A_{22} \end{bmatrix} \begin{bmatrix} E_{//i} \\ E_{\perp i} \end{bmatrix} \tag{3}
$$

Eq.(3) can used with two cases for an incident electric field to obtain calculatable expressions for the A_{ij} in terms of the incident and scattered electric field components. For example, when we use incident left and right circularly polarized light, defined by $E_L = E_0(e_x + i\,e_y)$ and $E_R = E_0(e_x - ie_y)$, the A_{ij} can be written;

$$
A_{11} = C[-i\{(E_{//s})_R + (E_{//s})_L\}] \qquad A_{12} = C[(E_{//s})_L - (E_{//s})_R]
$$

$$
A_{21} = C[-i\{(E_{\perp s})_R + (E_{\perp s})_L\}] \qquad A_{22} = C[(E_{\perp s})_L - (E_{\perp s})_R] \tag{4}
$$

where $C = 2\exp(ik(r-z))/kr$. We are considering a static case, so the time-dependence is not shown here. The elements of the Mueller matrix can be determined in terms of the A_{ij} by algebraic manipulation. Expressions for the 16 elements of the matrix can be found in Bohren and Huffman.[1]

Experimental methods for determining the Mueller matrix elements generally involve selecting incident light with a particular polarization state and measuring the total intensity, I, of the scattered light. The element S_{11} is proportional to the total intensity of the scattered light. The normalized matrix element S_{14}, a measure of the ability of the scatterer to differentially scatter right vs. left circularly polarized light, is given by:

$$S_{14} = \frac{S_{14}}{S_{11}} = \frac{I_R - I_L}{I_R + I_L} \tag{5}$$

where I_R is the intensity of scattered light from incident right circularly-polarized light and I_L is the intensity of scattered light from incident left circularly-polarized light. S_{14} is also a measure of the ability of a scattering medium to depolarize circularly-polarized light. As circularly polarized light is useful in enhancing visibility in the ocean, it is important to understand those circumstances under which oceanic conditions might result in (unexpected) depolarization. Because of symmetry, this matrix element is identically zero for spherically-shaped objects or collections of randomly-oriented non-spherical particles that are not optically active on a molecular scale. However, even in the absence of a molecular-scale optical activity, S_{14} is non-zero for collections of non-spherically-symmetric particles possessing some degree of alignment, or organisms with chiral symmetry. Such conditions can be expected if organisms found to have non-zero S_{14} are present in significant quantity, particularly if they are aligned.
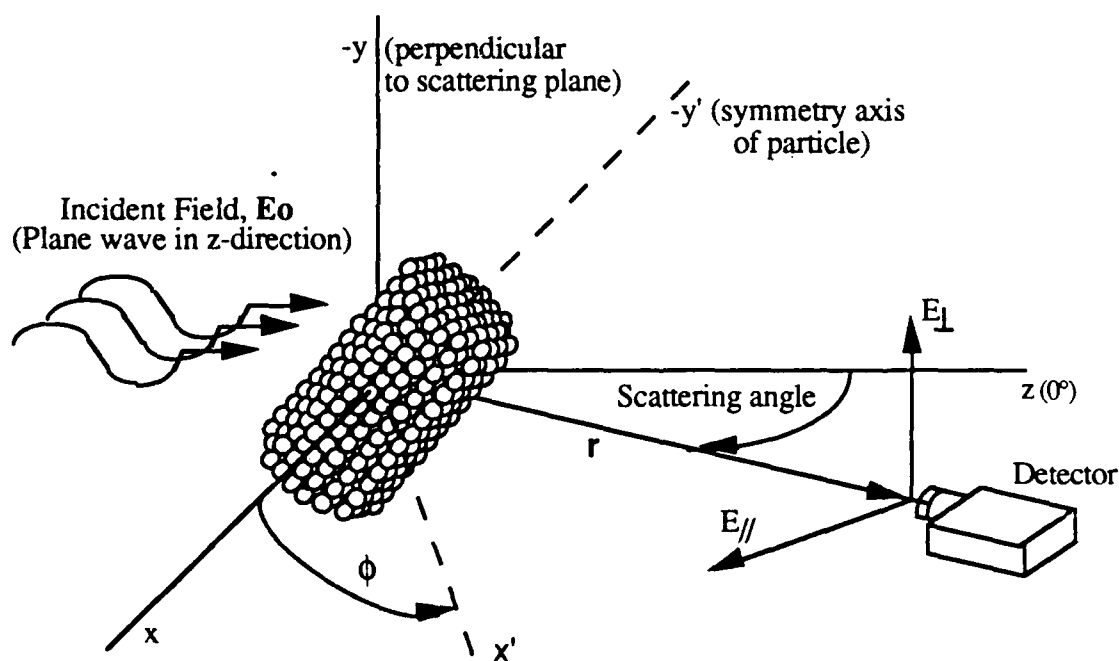

Figure 1. Geometry of the particle orientation and scattering plane

THE COUPLED DIPOLE METHOD

In order to describe the scattering of light from marine organisms of other than the simplest shapes (*i.e.* spheres, very long cylinders), it is necessary to resort to approximate methods. In an earlier paper, Hunt and Quinby-Hunt[2] compared the Rayleigh-Debye approximation with Mie calculations for predicting the scattering by nearly spherical marine organisms. The Rayleigh-Debye approximation can be extended to various shapes, but predicts zero for all matrix elements but those that are non-zero in the Rayleigh limit, S_{11}, S_{12}, and $S_{33}(=S_{44})$. The Rayleigh-Debye model is therefore not useful for understanding depolarization of circularly polarized light. The coupled-dipole model, developed by Purcell and Pennypacker[3] in 1973, has been chosen for this project because an organism of any shape can, at least in principle, be modelled, and all sixteen elements of the Mueller scattering matrix can be calculated and are generally non-zero. In this model, an arbitrarily-shaped object is divided into a number of identical units arranged on a cubic lattice. A sketch of various geometric shapes modelled by spherical units is shown in figure 2. Each unit is treated as a spherical, dipolar oscillator. Interactions between dipoles are included by determining the field at a particular dipole due to the incident field and the fields induced by the other dipole oscillators. If there are m such dipolar oscillators, the field at a dipole i, E_i, is due to the incident radiation, E_0, as well as contributions from the other dipole oscillators, *i.e.*,

$$E_i - \sum_{\substack{j=1 \\ j \neq i}}^{m} \left(\frac{e^{ikr_{ij}}}{r_{ij}} \right) \left[\left(k^2 - \frac{1}{r_{ij}^2} + \frac{ik}{r_{ij}} \right) \alpha_j E_j + \left(\frac{3}{r_{ij}^2} - k^2 - \frac{3ik}{r_{ij}} \right) (\alpha_j E_j \cdot n_{ji}) n_{ji} \right] = E_0 e^{ik \cdot r_i} \qquad (6)$$

where α_j is the complex polarizability tensor, k is the wave number of the radiation, r_{ij} is the distance from the ith to the jth dipole and n_{ji} is a unit vector along r_{ij}. The above equation represents a system of $3m$ linear equations with complex coefficients with $3m$ unknown components of the electric fields, E_i (3 at each dipole location). Once this system of equations has been solved, the scattered electric field, E_d, at a detector far from the object is given by;

$$E_d = \frac{k^2 e^{ikr_d}}{r_d} \sum_{j=1}^{m} e^{-ikn_d \cdot r_j} \left[\alpha_j E_j - (\alpha_j E_j \cdot n_d) n_d \right] \qquad (7)$$

where r_d is the distance from the origin to the detector, r_j is the distance from the origin to the jth dipole and n_d is a unit vector along r_d. The 16 elements of the Mueller matrix are ther calculated from the electric field components perpendicular and parallel to the scattering pla e. In 1986, Singham and Salzman[4] used the coupled-dipole method to calculate the matrix elements for scattering from a solid sphere and a hollow spherical shell. They reported excellent agreement with the Mie calculations for size parameters of 0.75 and 1.50, but noted that a greater number of computer calculations would be necessary to achieve good results for larger size parameters.
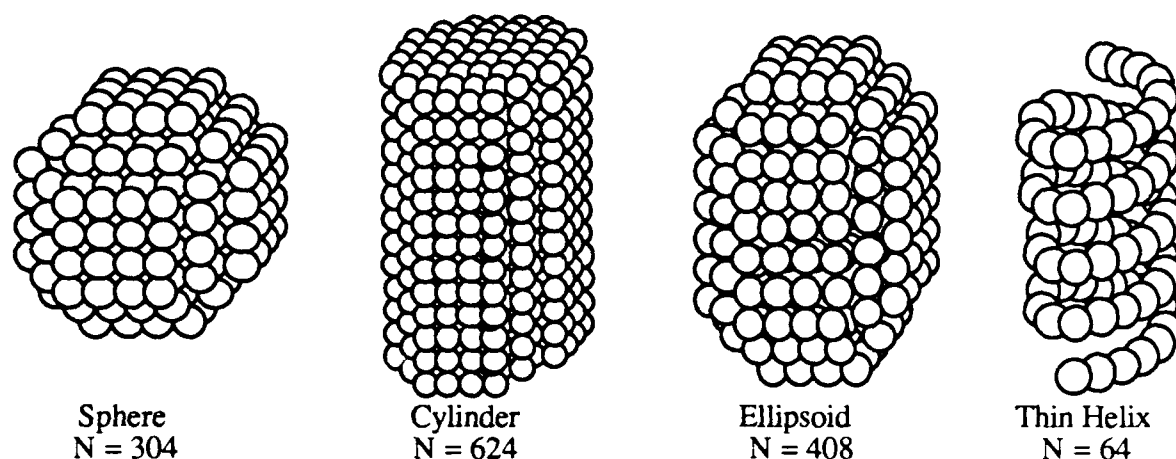
Figure 2. Sketch of various geometric shapes modelled with spherical units.

4. TASKS COMPLETED

The inversion of the $3m \times 3m$ matrix necessary to solve for the E_i in Eq. (5) is a formidable task for a computer both in terms of storage requirements and processing time. We have employed two methods for inverting the matrix; (1) a direct inversion using the Cyber 205 'super' computer, and (2) a technique for matrix solution developed by Singham and Bohren[5], a scattering order approximation. The computations necessary in the scattering order approximation were done on a micro-VAX 2000. We applied both the scattering order and direct inversion methods to calculate the scattering from spherical particles to determine the limits of the approximations. For large size parameters, the total intensity (S_{11}) calculated by the two approximation methods differed significantly from each other and the values for spheres using Mie calculations, particularly for large scattering angles. The results were in good agreement for size parameters up to about 6. For visible light, the largest sphere that could safely be modelled was 500nm in radius with up to 2000 dipoles, although with greater than 2000 dipoles the calculations became excessively long on the micro-VAX. A critical factor in the scattering order approximations method was the size parameter of the spherical dipole rather than the bulk object. When the size parameter of the spherical dipole was greater than 0.5, agreement of the scattering order approximation with Mie calculations declined, particularly at high scattering angles. It is not necessary to keep the dipoles small in the direct inversion method, but the available storage on the Cyber for a direct inversion of the $3m \times 3m$ matrix limited the number of dipoles that could used to model a shape to about 500.

Both approximation methods were applied to other shapes to investigate the effects of non-sphericity and chirality on scattering. In particular, all 16 Mueller matrix elements were calculated for the scattering of light from a cylinder, a single-strand helix, a 14-strand helix, and ensembles of these particles. Input parameters for the computer programs included particle shape and dimensions, wavelength of the incident light, index of refraction of the medium, orientation and complex index of refraction of the particle. The effects of particle size and wavelength are not independent and are usually presented in terms of an appropriate size parameter. We defined the size parameter of a cylinder to be 2π times an 'equivalent sphere' radius divided by the wavelength

of the incident light in the medium; where an 'equivalent sphere' is a sphere having the same volume as the cylinder of interest. In order to give the reader a more 'physical' interpretation, the wavelength was fixed at 500nm and the particle dimensions were varied. The medium, sea water, had an index of refraction of 1.34. We made a number of calculations for a single particle using both methods in which we varied particle dimensions, complex index of refraction for the particle, and orientation of the particle with respect to the incident light. We also calculated the Mueller matrix elements for collections of particles (cylinders and thin helices) using only the scattering order approximation. The size of the collection was kept small in these calculations because of the large computational time required.

5. RESULTS

The results of the computer computations are best presented graphically. In the interest of simplicity, we have limited the graphs for a single particle and collections of particles to the normalized S_{14} Mueller matrix element as this element is associated with the depolarization of circularly-polarized light. The effects on the S_{14} element for scattering from a single cylinder for changes in size are shown in figure 3. The dramatic effect on S_{14} when the particle is large compared to the wavelength of the incident light is not particularly surprising and is consistent with the analytical results for the infinite cylinder at an oblique angle with respect to incoming light. The graphs are included because an understanding of how particle size affects S_{14} is important in differentiating between effects due to size and those due to orientation or asymmetries in shape.
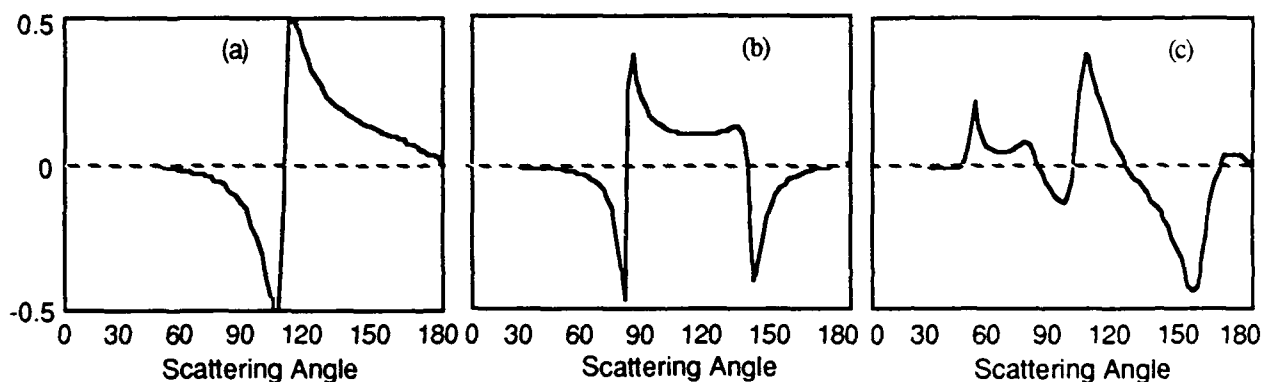

Figure 3. Variations in the normalized Mueller matrix element, S_{14}, for a single cylinder oriented at Euler angles of $\phi=30°$ and $\theta=30°$ as size parameter is increased. The length to diameter ratio of the cylinder is 1.6. Graphs (a), (b), and (c) are for size parameters as defined in the text of 1.96, 2.56, and 5.0, respectively. A size parameter of 5.0 corresponds to a cylinder with a radius of 300 nm and a length of 960 nm for incident light with a wavelength of 500 nm. The cylinders were modelled by 290 dipoles.

S_{14} for a 14-strand helix similar to the structure of deoxyhemoglobin described by Noguchi and Schecter[6] is shown in figure 4. The diameter and length of the helix as modelled was 64nm and 320nm, respectively. The graphical results shown in figure 4(a) demonstrates that changes in the optical properties of the helix tend to change the height and broadness of the peaks but leaves their positions unchanged. On the other hand, as demonstrated in figure 4(b), changes in its physical properties change the number and positions of the peaks. Altering the pitch of the helix had little

effect, but the dense packing of the structure tended to make the helix behave much like a cylinder of similar dimensions and orientation.
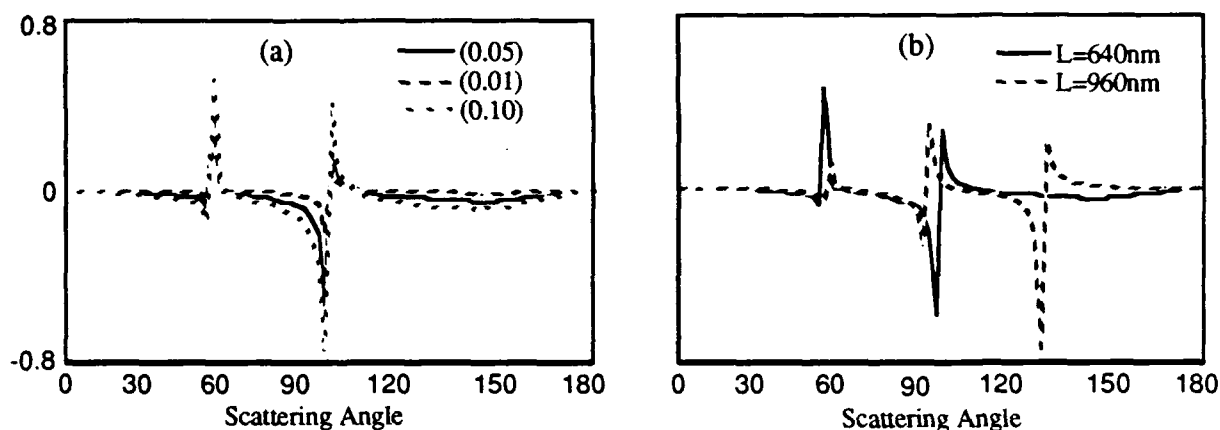

Figure 4. S_{14} for a 14-strand thick helix with a diameter of 64nm, pitch of 320nm and relative real index of refraction of 1.05, oriented at Euler angles of 30°, 45°. Graph on the left shows the effects in S_{14} as the imaginary part of the relative index of refraction is varied while keeping the length constant at 640nm. Graph on the right shows the effects on S_{14} as the length, L, of the helix is varied while keeping the pitch constant at 320nm and relative complex index of refraction constant at 1.05+0.05i. (Same helix is represented by solid line in both graphs.)

The particle's orientation is determined by a rotation of the particle's principal axes through the Euler angles ϕ, θ and ψ. Angle ϕ is a counterclockwise rotation about the z-axis, θ is a counterclockwise rotation about the new x-axis and ψ is a counterclockwise rotation about the new z-axis. The orientation of the particle after the rotation depends on the initial position of the particle with respect to the laboratory coordinate axes. The angle, ϕ, in the laboratory frame for the initial alignment of a cylinder along the y-axis is shown in figure 1. The angle, θ, is more difficult to show in this figure. Euler rotations are described in Goldstein[7] if the reader is interested in a more detailed discussion. The value of ψ was zero for all cases and we have dropped it in the subsequent notation. S_{14} for several different orientations of a single cylinder is shown in figure 5. The variations in S_{14} as the cylinder's orientation is changed suggest some degree of alignment of micro-organisms plays a significant role in the depolarization of incident light. The effects of orientation tend to cancel, however, when S_{14} is averaged for randomly-oriented collections of particles. In order to demonstrate the effect of partial alignment of a collections of particles, we calculated the average S_{14} for a cylinder, summing the contributions from cylinders oriented from ϕ from 0 to π and over θ from -π/6 to π/6. Figure 6(a) shows that the average S_{14} we calculated for this collections of cylinders is non-zero. Note that the average S_{14} for a uniformly distributed collection shown in figure 6(b) is also non-zero but small, generally less than 1% of the total intensity. The non-vanishing S_{14} is apparently a cylinder 'edge' effect that exaggerates the error inherent in averaging over a small sample. The average S_{14} matrix elements calculated for collections of spheres and ellipsoids (modelled from approximately the same number of dipoles) were zero to within one part in ten thousand for all scattering angles. (Compare the ellipsoid and cylinder shown in figure 2 for an indication of the 'bumpiness' of each shape.) A number of calculations demonstrated that increasing the number of dipoles, while leaving the number of cylinders in the collection constant, did not tend to result in a zero average S_{14}. On the other hand,

keeping the number of dipoles constant, but increasing the number of cylinders resulted in average S_{14} values that tended to zero. We concluded that the 'bumpiness' of the model due to number of dipoles is less important when averaging over collections of particle than the number of particles in the collection.

Figure 7 shows the results of calculations of S_{14} for collections of single-strand helices similar to that illustrated in figure 1. The calculations sum the results of the contributions from a large number of single strand helices uniformly distributed over the Euler angles ϕ and θ. The figure contrasts the results for collections of all right-handed and all left-handed helices. Note that the curves are generally the negative of each other and reach a maximum value of S_{14} less than 4%. That the two curves are not exactly opposite from each other (as anticipated for symmetry reasons) is probably due to two primary factors. First, the calculation for the right-handed case was done with a later version of the computer program that had twice the angular resolution of the left-handed case, so that some details are different. Second, no averaging was performed about the axis of the helices. Calculations of S_{14} for short helices of this type showed significant differences depending on the starting rotational position of the helical strand. Thus, the lack of averaging about the axis may account for the differences. Shapiro and others[8] interpreted their experimental measurements of induced circular polarization in the light scattering from a marine dinoflagellate as being due to the helical structure of the organism's chromosomes. The single-strand helix showed much stronger changes in S_{14} when physical properties, such as orientation, were changed than the 14-strand (thick) helix.
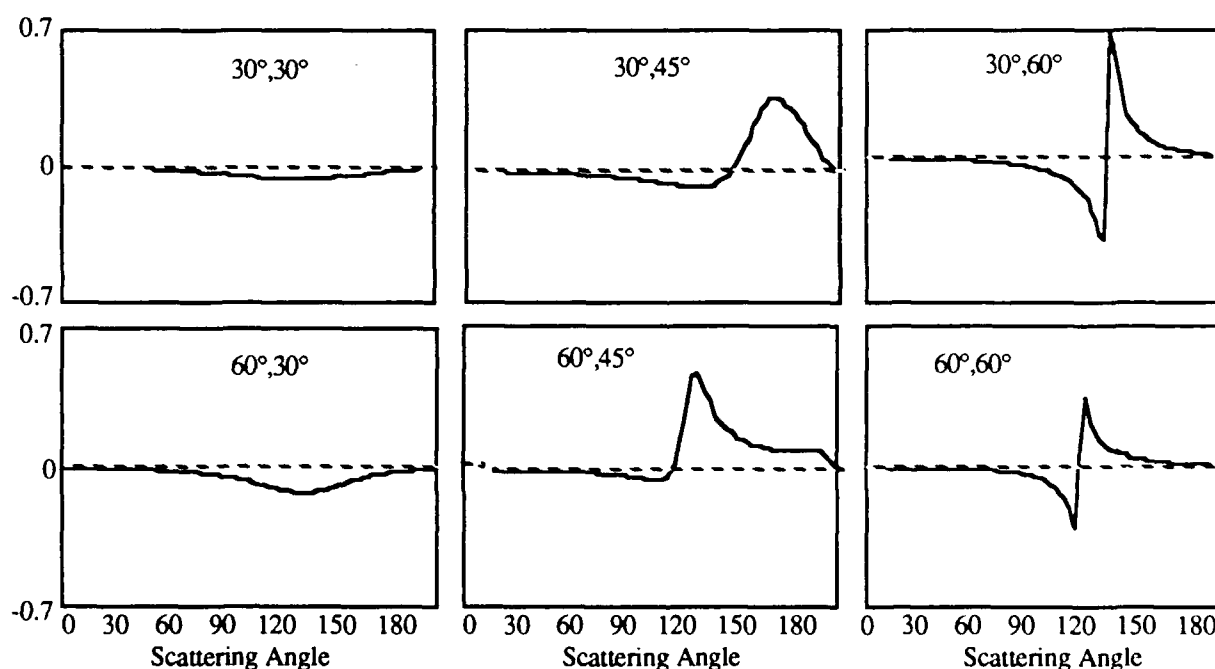

Figure 5. The normalized S_{14} matrix element for a cylinder with a complex index of refraction of 1.05+.05i and a size parameter of 1.33 (radius=90nm,length=1440). The angles shown on the graph are Euler angles, θ, and ϕ. At angles 0°,0° the cylinder axis is along the laboratory y-axis, orienting the cylinder at right angles both to the incoming light and the scattering plane.
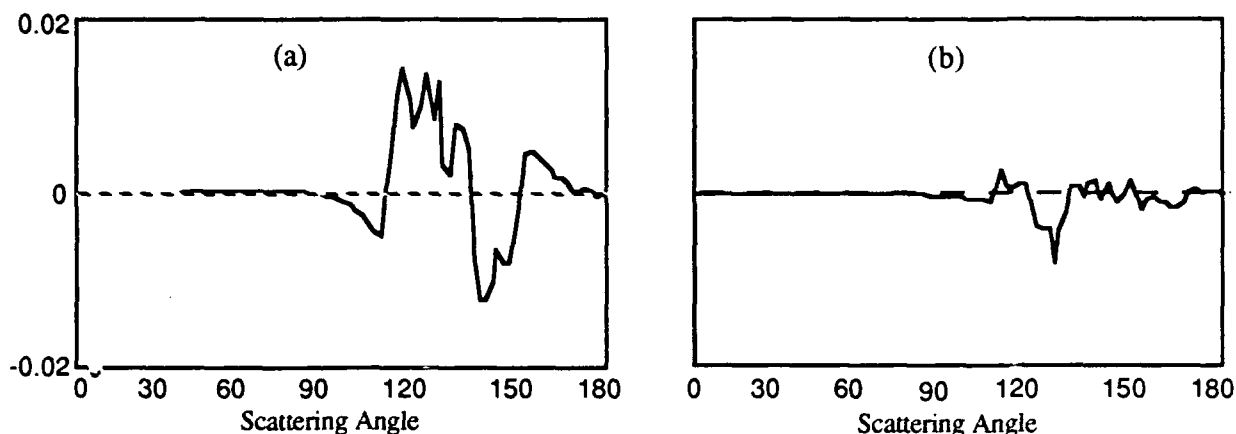
Figure 6. The Mueller matrix element S_{14} for collections of cylinders. The graph on the left was produced when the S_{14} element for a set of identical cylinders with a size parameter of 1.33 (radius=90nm, length=1440nm) and complex index of refraction of 1.05+.05i was averaged over the non-uniform distribution described in the text. The graph on the right was produced when S_{14} for the same set of cylinders was averaged over a uniform spatial distribution. Each cylinder was modelled with 168 dipoles and S_{14} averaged for 1296 orientations of the cylinder.
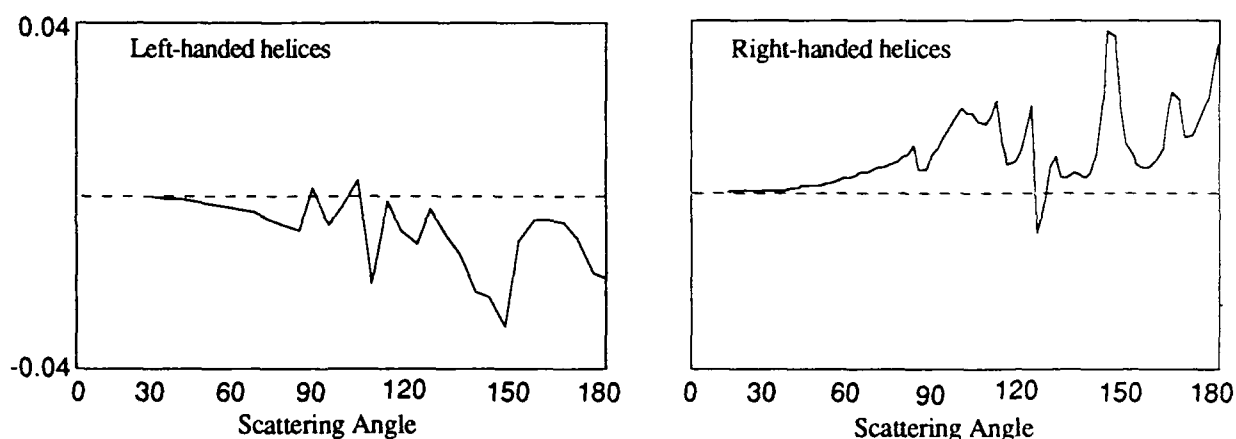

Figure 7. The S_{14} Mueller matrix element for a collection of (identical) uniformly oriented single-strand helices. Each helix was modelled with 162 dipoles. For incident light with a wavelength of 500 nm, each helix has a thickness of 50 nm, a radius and pitch of 250 nm and a length of 1250 nm. The average value was calculated for 1296 orientations of each helix.

In summary, the results of the calculations in this study showed that: (1) Increasing the size of the particle increased the complexity of angular scattering; (2) varying the complex index of refraction affects the intensity of S_{14} for thick helix, but not its complexity; (3) small changes in the orientation of a non-spherical particle have a large effect on S_{14}; (4) left and right-handed helices scatter light differently; and, (5) averaging the results over cylinders with many orientations does not rapidly converge to the zero result expected; possibly due to the small number of cylinders used in the averaging process. The dipoles in the scattering order method had to be kept relatively small (size parameter less than 0.5), therefore, modelling larger objects required very large numbers of dipoles. If more than 2000 dipoles were used, the computation time on the micro-VAX became excessively long. The elements of the Mueller matrix could be calculated with the Cyber for

particles with large size parameters as long as no more than 500 dipoles were used, but the bumpiness of the model produced less reliable results.

6. ACCOMPLISHMENTS

Agreement of our calculations with rigorous (Mie) calculations for a sphere suggests that the coupled-dipole method is a viable technique for determining light scattering from non-spherical particles. Since very little work is being done in predicting the behavior of polarized light in sea water, this work is a valuable contribution in a number of areas in which polarized light plays an important role.

7. PRESENTATIONS

Hull, P., Hunt, A., Quinby-Hunt, M., and Shapiro, D. 1991: An analytical model for predicting light scattering from marine micro-organisms, Proc. **SPIE**, 1537.

Shapiro, D., Hunt, A., Quinby-Hunt, M., and Hull, P., 1991: Circular polarization effects in the light scattering from single and suspensions of dinoflagellates, Proc. **SPIE**, 1537.

8. REFERENCES

1. C.F. Bohren and D.R. Huffman, *Absorption and Scattering of Light by Small Particles*, John Wiley & Sons, New York, 1983.
2. M.S. Quinby-Hunt and A.J. Hunt, "Effects of Structure on Scattering from Marine Organisms: Rayleigh-Debye and Mie Predictions," *Proc.Ocean Optics IX.* SPIE, 288-295, 1988.
3. E.M.Purcell and C.R. Pennypacker, "Scattering and Absorption of Light by Nonspherical Dielectric Grains," Astrophy. J. Vol.**186**, 705, 1973.
4. S.B. Singham and G.C. Salzman, "Evaluation of the Scattering Matrix of an Arbitrary Particle Using the Coupled-Dipole Approximation," J. Chem. Phys. **84**, No.5, March 1986.
5. S.B.Singham and C.F. Bohren, "Light Scattering by an Arbitrary Particle: the Scattering Order Formulation of the Coupled-dipole Method," J. Opt. Soc. Am. A Vol.**5**, No.11, p.1867, 1988.
6. T. Noguchi and A. Schechter, "Sickle Hemoglobin Polymerization in Solution and in Cells," Ann. Rev. Biophys. Chem. Vol.**14**, p.239, 1985.
7. H. Goldstein, *Classical Mechanics*, Addison Wesley, Reading, MA, 1959.
8. D. Shapiro, A.Hunt, and M.Quinby-Hunt, "Origin of the induced Circular Polarization in the Light Scattering from a Dinoflagellate," *Proc. Ocean Optics X*, Orlando, FL., April 1990.

7. ACKNOWLEDGMENTS